Analytical Biochemistry 546 (2018) 5–9

Contents lists available at ScienceDirect

Analytical Biochemistry

journal homepage: www.elsevier.com/locate/yabio

Zeolitic imidazolate framework-based biosensor for detection of HIV-1 DNA

Yong Pan[a,**], Shenshan Zhan[a], Fan Xia[a,b,*]

[a] Hubei Key Laboratory of Bioinorganic Chemistry & Materia Medica, School of Chemistry and Chemical Engineering, Huazhong University of Science and Technology (HUST), 1037 Luoyu Road, Wuhan 430074, China

[b] Faculty of Materials Science and Chemistry, China University of Geosciences, Wuhan 430074, China

ARTICLE INFO

Keywords:
Biosensor
HIV-1 DNA
Zinc-methylimidazolate framework-8

ABSTRACT

ZIF-8(zinc-methylimidazolate framework-8), one of the zeolitic imidazolate frameworks (ZIFs), as quenching platforms for detection of HIV-1 DNA, which was identified to be effective for highly sensitive detection of HIV-1 DNA. The enhanced fluorescence signal has a relationship with the ssDNA concentration, the detection limit is as low as 1.2 nmol L^{-1} with good selectivity. This study is an important step toward rational design of materials to achieve specific interactions between biomolecules and synthetic particle surfaces.

Introduction

The Human Immunodeficiency Virus (HIV) is a deadly virus which infects many people worldwide. Often, the virus can present inside a subject for many months before being detected. This property of the HIV virus, which is asymptomatic inside the human body for long time, is the main reason for the wide spread of the virus. According to the recent statistics, 36.9 million people worldwide are living with HIV, 2 million were newly infected, and 1.6 million died [1–4]. This number of infected people clarifies the need of increased awareness about this virus and the need to find a proper method capable of detecting HIV earlier in order to prevent the spread of the virus.

There are many kinds of HIV virus detection methods available, such as the HIV antibody test, P24 antigen test, Nucleic acid detection, Test paper detection and HIV Viral Load test. However, their further applications suffer from high cost, risk of contamination and false negative results [5–8]. Therefore, it is in urgent need to develop a new, simple, fast, sensitive and low-cost method for the detection of HIV DNA.

At present, Various types of biological probes have been developed to detect DNA sequences, this method has also been paid much attention by most researchers, The fluorescence detection of nuclei acids based on fluorescence resonance energy transfer (FRET) or a quenching mechanism with fluorescently-labeled nuclei acids has been widely developed [9–13]. Numerous materials have been employed as quenching platforms to detect DNA sequences, including coordination polymers [14], macroporous silicon [15], carbon nanomaterials (CNMs) [16–18] etc. Chen employing metal–organic frameworks (MOFs) as quenching platforms for the detection of proteins and nucleic acids based on fluorophore-labeled oligonucleotide probes for the first time [19–21].

As a unique class of hybrid nanoporous materials, MOFs are materials which consist of metal ions or clusters connected by organic linker groups, and have attracted considerable interest in recent years owing to their potential in gas storage and separation, catalysis, and other emerging applications [22–25]. Zeolitic imidazolate frameworks (ZIFs) are a sub-family of MOFs that also have tunable pore sizes and chemical functionality [26]. Moreover, ZIFs possess the exceptional chemical stability and rich structural diversity found in zeolites. ZIFs are based on metal imidazolates, and their structures are similar to the SiO_2 frameworks of silicate zeolites [27,28].

In this study, we utilize as-synthsised ZIF-8 as the sensing platform to detect ss-DNA (HIV 20-bp oligopyrimidine·oligopurine proviral DNA) in vitro. The results demonstrated that the adsorption is primarily brought about by a specific favorable interaction (electrostatic interaction) between ss-DNA and ZIF-8 surface. The schematic diagram of this senor is shown in Scheme 1. ZIF-8 contains stacking Π-electron systems of the bridging five-membered imidazolate ring, which strongly adsorbs fluorophore carboxyfluorescein (FAM)-labeled single-stranded DNA (ss-DNA) through Π-Πstacking and quenches fluorescence of FAM due to the photoinduced electron transfer (PET) process [29]. Meanwhile, the electrostatic interaction can not be ignored, electrostatic interaction and Π-Πstacking interaction are together contributed to the whole process of adsorption. After addition of the complementary ss-DNA, the probe DNA interacted with the bases of the target ss-DNA to form a ds-DNA, the probe DNA is desorbed from ZIF-8 and the

* Corresponding author. Hubei Key Laboratory of Bioinorganic Chemistry & Materia Medica, School of Chemistry and Chemical Engineering, Huazhong University of Science and Technology (HUST), 1037 Luoyu Road, Wuhan 430074, China.

** Corresponding author.

E-mail addresses: m13051792239@163.com (Y. Pan), xiafan@hust.edu.cn (F. Xia).

https://doi.org/10.1016/j.ab.2018.01.017
Received 7 November 2017; Received in revised form 16 January 2018; Accepted 19 January 2018

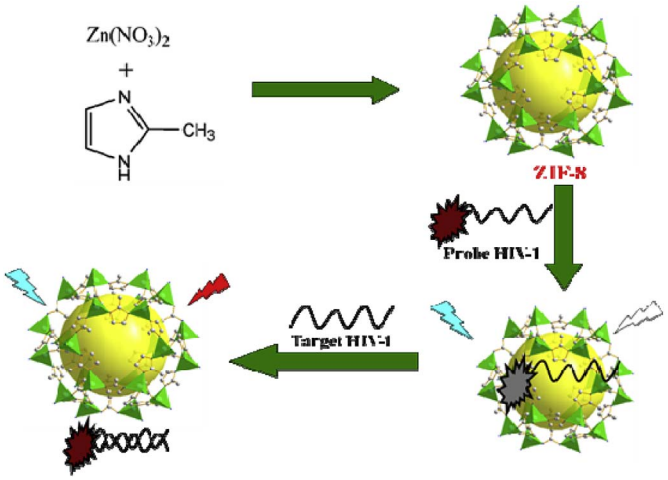

Scheme 1. Mechanism for the target HIV DNA fluorescent biosensor based on ZIF-8.

fluorescence of the probe DNA is recovered, Enhancement of the fluorescence intensity is related to the concentration of the target ss-DNA.

Experimental

Materials and physical measurements

Zinc nitrate hexahydrate ($Zn(NO_3)_2{\cdot}6H_2O$) (purity 99.8%, Sigma-Aldrich), 2-methylimidazole (purity 99.8%, Sigma-Aldrich), Deionized water (H_2O, home-made), were used as obtained from commercial sources and used without further purification.

The human imunodeficiency virus (HIV)-1 U5 long terminal repeats (LTR) DNA and other ssDNA were synthesized and purified by Sangon Biotechnology Co. Ltd (shanghai, china), and all DNAs were used without further purification. The sequence of the probe DNA (P) was 5′-AGT CAG TGT GGA AAA TCT CTA GC-3′, with 6-carboxyfluorescein (FAM)-labeled at 5′-terminal. The sequence of the complementary target DNA (T_0) was 5′- GCT AGA GAT TTT CCA CAC TGACT-3′. Mismatched oligomers were employed to confirm the specificity of our strategy, including, one-base-mismatched oligomer (T1), 5′- GCT AGA GAT TTT *A*CA CAC TGA CT-3′; two-base-mismatched oligomer (T2), 5′- GCT AGA GAT TTT *A*CA CAC T*A*A CT-3′; three-base-mismatched oligomer (T3), 5′- GCT A*T*A GAT TTT *A*CA CAC T*A*A CT-3′.

All the samples were dissolved in 100 nM Tris-HCl buffer solution (pH 7.2, 100 mM NaCl, 5 mM $MgCl_2$). DNA was stored at 4 °C for use.

All the other reagents and solvents were obtained from commercial sources and used without further purification. All the instruments used for the detection of DNA sequences were sterilized in an autoclavable container.

Powder X-ray diffraction (PXRD) spectra were recorded with a Rigaku 2500 VBZ + /PC. The X-ray generated from a sealed Cu tube was monochromated by a graphite crystal and collimated by a 0.5 mm MONOCAP (λ Cu-Kα = 1.54178 Å). The tube voltage and current were 40 kV and 40 mA, respectively. Thermogravimetric analysis (TGA) was performed on a PerkinElmer Pyris Diamond TG Thermogravimetric Analyzer at a heating rate of 10 °C min^{-1} under a nitrogen gas flow in an Al_2O_3 pan. Nitrogen physisorption isotherms were measured at 77 K, on a Quantachrome Autosorb Automated Gas Sorption instrument. Infrared spectra were acquired from a Nicolet 6700 FTIR-ATR (Fourier Transform Infrared Spectroscopy-Attenuated Total Reflectance) spectrophotometer. Fluorescence spectra were measured on an Cary Eclipse fluorescence spectrophotometer. Zeta potential measurement was carried out on a NanoZS 90 zetasizer. PHS-3CPH pH meter (Shang Hai, China) was employed to adjust the pH values.

Synthesis of adsorbents

ZIF-8 was synthesized using 2-methylimidazole as a linker according to the previously reported protocol [30,31]. The synthesis solution, which had a molar ratio of Zn^{2+}:2-methylimidazole:H_2O = 1:8:1000, was prepared as follows: First, 6.56 g of 2-methylimidazole was dissolved in 120 mL of DI water, and the pH of the solution was adjusted to approximately 9.5 using TEA. Second, 2.95 g of Zn $(NO_3)_2{\cdot}6H_2O$ was dissolved in 60 mL of deionized (DI) water. Then, the Zinc nitrate solution was mixed with the 2-methylimidazole solution under stirring. All of the operations were performed at room temperature (20 ± 2 °C). After stirring for 20 min, the reaction solution was delivered to a filter using an air compressor. Then, the solution was filtered and washed with (DI) water several times. To accelerate the filtration rate of the entire process, the system was pressurized using nitrogen. Finally, a product was obtained. The as-synthesized product contains large amounts of 2-methylimidazole and water. The activation procedure leading to a clean, empty and stable material was achieved using the following in-house procedure. Excess 2-methylimidazole and pore-occluded water were completely removed by sonification of the microcrystalline product three times in deionized water for 2 h. Then, the ZIF-8 sample was heated to 120 °C under vacuum for 3 days to remove the solvents and other guest molecules in the pores. The yield of ZIF-8 was 1.804 g. The resulting void-cleaned sample is referred to as the “activated sample”.

Fluorescence measurements

Briefly, 50 μL of Tris-HCl buffer (pH 7.2), 25 μL of NaCl solution (3 M), 100 μL of FAM-labeled probe DNA (100 nM) and 75 μL of ZIF-8 solution (3 mg/mL) were sequentially added into a 1.5 mL tube, and kept at room temperature (25 °C) for 60 min. The fluorescence intensity of the solution was detected. Later on, a certain volume of target DNA (0.1 μM) was added into the mixture and further diluted with ultrapure water to 500 μL. After 120 min incubation at 35 °C, fluorescence measurements were carried out on the Cary Eclipse fluorescence spectrophotometer with an excitation wavelength of 480 nm and emission intensity at 520 nm was recorded.

Results and discussions

Characterization of the as-synthesized ZIF-8 adsorbents

ZIF-8 was synthesized in 79% yield from the reaction of Zn $(NO_3)_2{\cdot}6H_2O$ with 2-methylimidazole in water at room temperature. ZIF-8 is moisture and water stable. The prepared ZIF-8 was characterized by PXRD, TGA, FT-IR and N_2 adsorption experiments. ZIF-8 particles were successfully prepared with pure phase as demonstrated by PXRD patterns in Fig. 1. The powder X-ray diffraction (PXRD) pattern of a fresh powder of ZIF-8 immersed in H_2O for one week is in agreement with that of the simulated one, indicating its bulk phase purity and water stability (Fig. 1). The IR data reveals that the bands at 3135 and 2929 cm^{-1} are attributed to the aromatic and the aliphatic C-H stretch of the imidazole, respectively(Supporting Information Fig. S1). The peak at 1584 cm^{-1} can be assigned as the C=N stretch mode specifically, whereas the intense and convoluted bands at 1350-1500 cm^{-1} are associated with the entire ring stretching. The bands in the spectral region of 900–1350 cm^{-1} are for the in-plane bending of the ring while those below 800 cm^{-1} are assigned as out-of-plane bending. Due to the limitation of our IR apparatus (i.e., for mid-IR measurements only), the most interesting Zn-N stretch mode which is expected at 421 cm^{-1} was not observed. The TGA traces in Fig. S2 reveals that the ZIF-8 are stable up to 500 °C. The BET surface area (pore volume) of framework was calculated with N_2 adsorption data in Fig. S3 and found to be 1408 m^2/g (0.627 cm^3/g) (Supporting Information Table S1). The pore size distribution (PSD) analyzed with HK method demonstrated the existence

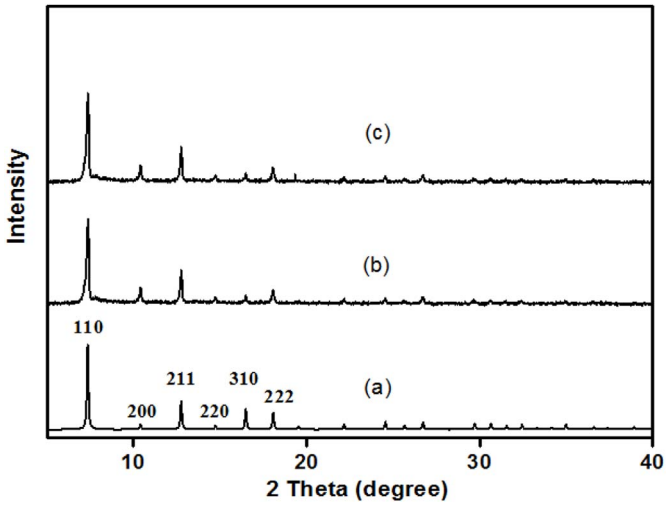

Fig. 1. PXRD patterns of ZIF-8 showing agreement between the simulated (a), synthesized (b) and fresh powder of ZIF-8 immersed in H_2O for 7 days (c).

of microporous in ZIF-8 framework. The average particle size of ZIF-67 was approximately 237.8 nm in Fig. S4.

Optimization of condition and dynamic studies of the sensor

In terms of the structures of ZIF-8, 2-methylimidazole usually contain a conjugated Π-electron system, be able to strongly interact with fluorophore carboxyfluorescein (FAM)-labeled single-stranded DNA (ss-DNA) through Π-Πstacking in theory, and then quench the fluorescence of FAM, which mechanism is similar to the interaction between GO and biomolecules. To test this, we chose FAM-5' -CATGTGTCCAGCTGATT GCC-3′ as a probe ss-DNA (P-DNA). As shown in Fig. 2(a), addition of ZIF-8 led to a decrease in the fluorescence intensity of P-DNA, suggesting that ZIF-8 can efficiently quench the fluorescence of P-DNA, possibly via the formation of a non-covalent complex. It is found that the fluorescence intensity decreases gradually until the concentration of ZIF-8 reaches 3 mg/mL, indicating saturation of the adsorption of P-DNA in the 60 min. The quenching efficiency (Q_E, %) of P-DNA is 66%, which was calculated according to the equation $Q_E\ \% = (F_0 - F_M)/F_0 * 100\%$, where F_M and F_0 are the fluorescence intensities at 520 nm in the presence and absence of ZIF-8, respectively. In this case, we calculate the molar ratio of Zn element to P-DNA is 97996:1. This high ratio may be due to the long chain of FAM-5′-CATGTGTCCAGCTGATTGCC-3′ bearing a large FAM tag with a diameter of 9.4 Å, which prevents P-DNA to enter the narrow six-membered-ring pore windows of 3.4 Å. Thus the pore of ZIF-8 cannot adsorb P-DNA efficiently. It may be adsorbed on the outsurface of ZIF-8 through Π-Πstacking.

Fig. 2(b) characterized the fluorescence emission spectra of the FAM-labeled ss-DNA as a function of incubation time with ZIF-8. Increasing the incubation time caused a gradual decrease in fluorescence intensity implying that more ss-DNA was adsorpted by ZIF-8.

Mechanisms of DNA-based biosensor

In order to gain further insight into the quenching properties of ZIF-8, we measured the quenching efficiency of $Zn(NO_3)_2$ and 2-methylimidazole (Hmin) toward P-DNA. The data are shown in Fig. 3 (a) and indicate that Hmin results in negligible fluorescence quenching (Q_E % = 1.3%). In contrast, the presence of $Zn(NO_3)_2$ led to significant quenching (Q_E % = 81.5%) with a saturation concentration of 1.5 mM. These results suggest that $Zn(NO_3)_2$ is also efficient in quenching the fluorescence of P-DNA. This may be a consequence of the intercalation of Zn^{2+} ions into the base pairs of P-DNA and the electrostatic binding with the phosphate back bones, triggering a photoinduced electron transfer (PET) process from FAM to Zn^{2+}. Through zeta potential measurement, we found that ZIF-8 is positive (+25.1 mV) when the pH is 7.4 (Supporting Information Fig. S5), and DNA is significantly negative due to phosphate the backbone, so an electrostatic interaction between ZIF-8 and P-DNA should not be negligible. Thus, it is reasonable to deduce that ZIF-8 can absorb P-DNA through electrostatic and p-stacking interactions to form the P-DNA@ZIF-8 complex [32–34], and thus quench the fluorescence of FAM, in which Zn^{2+} may play a critical role in triggering photoinduced electron transfer (PET) from FAM to Zn^{2+} (Scheme 1). Acoording to the experimental results, the time needed to reach stable quenching is 60 min (see Fig. 2(b)), We can theorize about that electrostatic interaction and Π-Π stacking interaction are together contributed to the whole process of adsorption, and the process of adsorption through Π-Π stacking interaction is the control step.

When the selected HIV-1 DNA sequences are complementary to the P-DNA sequence, they can form a stable DNA duplex. Thus, the addition of complementary HIV-1 DNA sequences to the P-DNA@ ZIF-8 or P-DNA@ $Zn(NO_3)_3$ system may compel P-DNA away from ZIF-8 or Zn $(NO_3)_2$, leading to fluorescence regeneration. In such a sense, the P-DNA@ ZIF-8 and P-DNA@$Zn(NO_3)_2$ systems can serve as sensing platforms for HIV-1 DNA. This hypothesis was tested by the fluorescence regeneration induced by the addition of HIV-1 DNA sequences (5′-GCT AGA GAT TTT CCA CAC TGACT-3′, T_0), a complementary target DNA to P-DNA. As shown in Fig. 3(b), the fluorescence is recovered upon addition of T_0 to the P-DNA@ ZIF-8 system. However, the fluorescence of the P-DNA@ $Zn(NO_3)_2$ system could not be recovered, presumably due to the strong interaction between Zn^{2+} ions and P-DNA. These results suggest that it is the unique structure of ZIF-8 that plays an essential role in fluorescence quenching and regeneration.

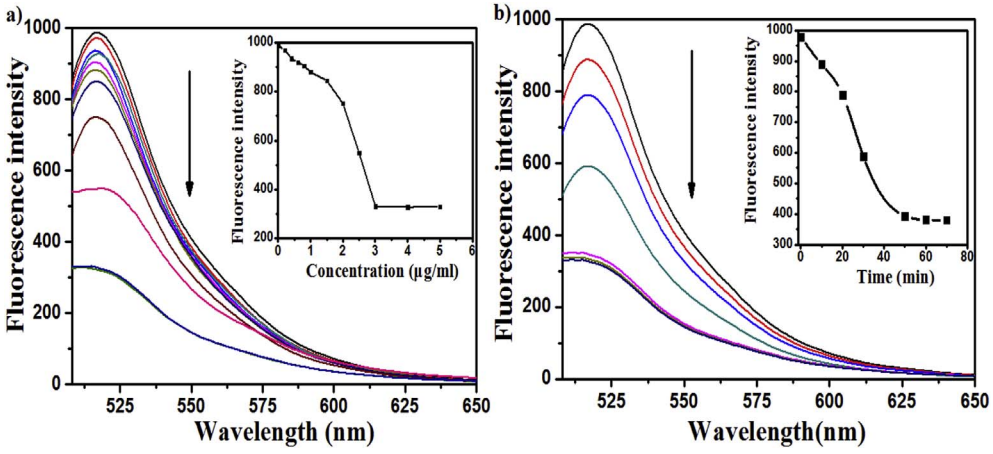

Fig. 2. (a) Fluorescence spectra of P-DNA (100 nM) incubated with ZIF-8 of varying concentrations in 10 mM Tris-HCl buffer (pH 7.2) at 25 °C. Inset: plot of the fluorescence intensity at 520 nm versus the concentrations of ZIF-8; (b) Fluorescence spectra of P-DNA (100 nM) with ZIF-8 of varying incubation time in 10 mM Tris-HCl buffer (pH 7.2) at 25 °C. Inset: plot of the fluorescence intensity at 520 nm versus incubation time.

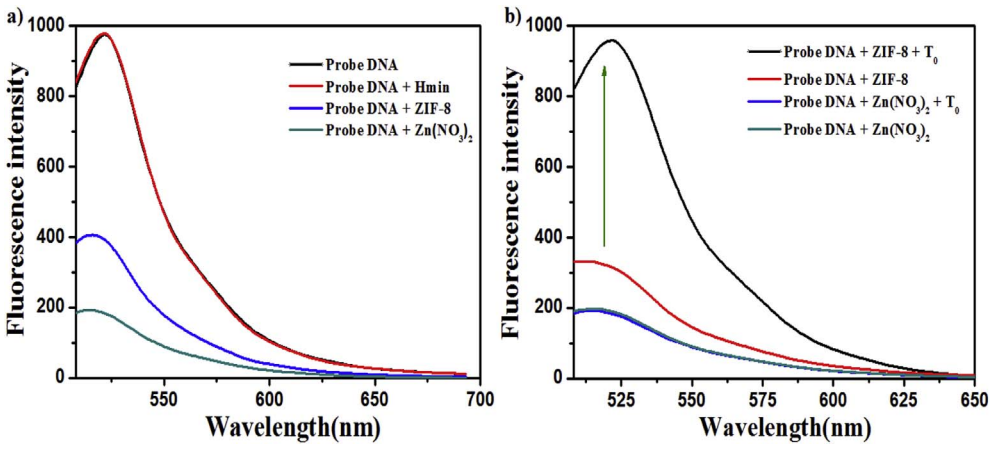

Fig. 3. (a) Fluorescence intensity of P-DNA (100 nM) by ZIF-8, Hmin and $Zn(NO_3)_2$ in 10 mM Tris-HCl buffer (pH 7.2) at 35 °C; (b) Fluorescence recovery of P-DNA (100 nM) @ ZIF-8 and P-DNA (100 nM) @$Zn(NO_3)_2$ system by T_0 in 10 mM Tris-HCl buffer (pH 7.2) at 35 °C.

Specifically, ZIF-8 forms a complex with P-DNA through multiple non-covalent interactions, in which Zn^{2+} ions play an important role in quenching the fluorescence of P-DNA. Such moderate interactions enable P-DNA to be released from the complex by forming a stable DNA duplex with T_0, leading to fluorescence regeneration. Thus, the P-DNA@ ZIF-8 system can be used as a highly effective fluorescent sensor for HIV-1 DNA sequences.

Quantitative analysis of the target ss-DNA

Fig. 4 shows fluorescence recovery efficiency (520 nm) of P-DNA@ ZIF-8 system by T_0 of varying concentrations, shows a linear relationship between the fluorescence intensity and the concentration of T_0 in the range 10 nM–100 nM with equation $(F_T - F_M)/F_M = 0.0189c_T + 0.0715$, $R^2 = 0.9974$ (Fig. 4, the inset). It is confirmed that the detection limit is as low as 1.2 nM ($3\delta_b$/slope, δ_b = standard deviation of fifteen blank measurements), which is lower than that of using single-walled carbon nanotubes (23 nM) as a nanoquencher-based DNA sensor [35], lower than that of using graphene oxide (14.3 nM) as the nanoquencher-based DNA sensor [36], the electrochemical-DNA sensor (10 nM) [37] and lower than that of using Cu-MOF (1.3 nM) as triplex DNA-based biosensor [38]. The fluorescence recovery efficiency (R_E) was 1.95, which was calculated using the formula $R_E = F_T/F_M - 1$, wherein F_T and F_M are the fluorescence intensities at 520 nm in the presence and the absence of T_0, respectively.

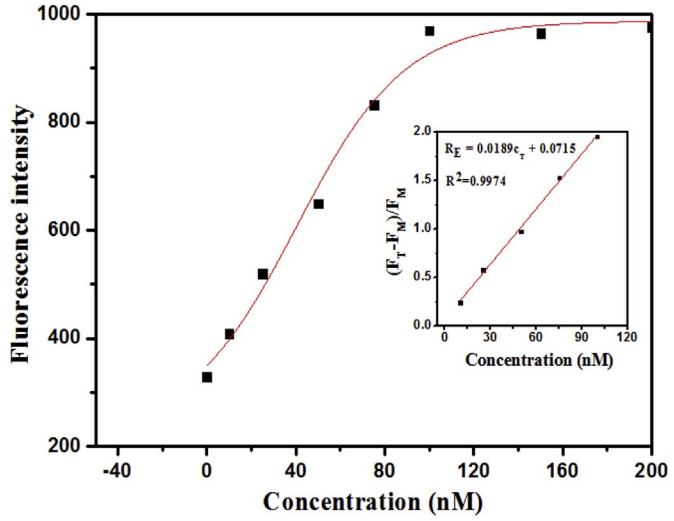

Fig. 4. Fluorescence recovery efficiency (520 nm) of P-DNA@ ZIF-8 system (100 nM/3 mg/mL) by T_0 of varying concentrations in 100 nM Tris-HCl buffer (pH 7.2). Inset: The plot of the fluorescence intensity at 520 nm versus the concentrations of T_0.

Sequence selectivity of the assay

In order to investigate the selective sensing ability of the P-DNA@ ZIF-8 system, we chose three different target DNAs, that is, one base pair mutated DNA T_1 (5′- GCT AGA GAT TTT *A*CA CAC TGA CT-3′), two-base-mismatched oligomer T_2 (5′- GCT AGA GAT TTT *A*CA CAC T*A*A CT-3′) and three-base-mismatched oligomer T_3 (5′- GCT A*T*A GAT TTT *A*CA CAC T*A*A CT-3′) to hybridize with P-DNA in the P-DNA@ ZIF-8 system. Under the same conditions, the R_E is 0.72 for T_1, 0.26 for T_2 and 0.13 for T_3, respectively (Fig. 5). In addition, T_0 shows much higher concentration-dependent fluorescence recovery than T_1, T_2 and T_3. These results indicate that the P-DNA@ ZIF-8 system can function as a highly selective sensing platform for the detection of HIV-1 DNA sequences in vitro.

Conclusions

In summary, we have successfully synthesized and characterized a moisture and water-stable ZIF-8. ZIF-8 can form Π-stacking interactions with P-DNA. The formed P-DNA@ ZIF-8 system can be used as an effective, selective and fluorescent sensing platform for the detection of HIV-1 DNA sequences. These findings may provide guidance for the synthesis of more Metal-organic frameworks with potential applications in the early diagnosis of HIV-1 DNA.

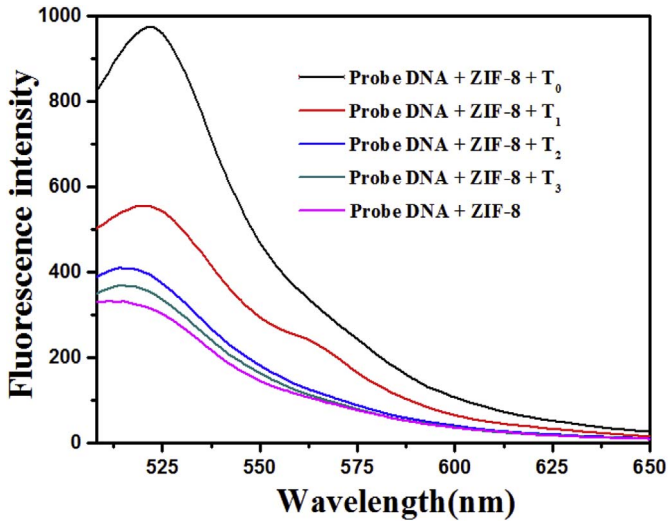

Fig. 5. Fluorescence recovery (520 nm) of the P-DNA@ZIF-8 system (100 nM/3 mg/mL) by T_0, T_1 and T_2 (100 nM).

Conflicts of interest

The authors have declared no conflict of interest.

Acknowledgements

This work is supported by National Basic Research Program of China (973 Program, 2015CB932600, 2013CB933000, 2016YFF0100800), the National Natural Science Foundation of China (21375042, 21405054, 21525523, 21574048), the National Key R&D Program of China (2017YFA0208000, 2016YFF0100800), The Fok Ying-Tong Education Foundation, China (151011), The China Postdoctoral Science Foundation (2017M622402), and 1000 Young Talent (to F.X.).

Appendix A. Supplementary data

Supplementary data related to this article can be found at http://dx.doi.org/10.1016/j.ab.2018.01.017.

References

[1] UNAIDS, How AIDS Changes Everything—MDG 6: 15 Lessons of Hope from the AIDS Response, (2015).
[2] F. Pereyra, X.M. Jia, P.J. McLaren, The major genetic determinants of HIV-1 control affect HLA class I peptide presentation, Science 330 (2011) 1151–1157.
[3] L.J. Sitole, A.A. Williams, D. Meyer, Metabonomic analysis of HIV-infected biofluids, Mol. BioSys. 9 (2013) 18–28.
[4] A. Engelman, P. Cherepanov, The structural biology of HIV-1: mechanistic and therapeutic insights, Nat. Rev. Microbiol. 10 (2012) 279–290.
[5] D. Desai, G. Wu, H.Z. Muhammad, Tackling HIV through robust diagnostics in the developing world: current status and future opportunities, Lab a Chip 11 (2011) 194–211.
[6] E.M. Gardner, M.P. McLees, J.F. Steiner, The spectrum of engagement in HIV care and its relevance to test-and-treat strategies for prevention of HIV infection, Clin. Infect. Dis. 52 (2011) 793–800.
[7] A. Gopi, S.M. Madhavan, S.K. Sharma, Diagnosis and treatment of tuberculous pleural effusion in 2006, Chest 131 (2007) 880.
[8] L.M. Zanoli, R. D'Agata, G. Spoto, Functionalized gold nanoparticles for ultrasensitive DNA detection, Anal. Bioanal. Chem. 402 (2012) 1759–1771.
[9] B. Dubertret, M. Calame, A.J. Libchaber, Single-mismatch detection using gold-quenched fluorescent oligonucleotides, Nat. Biotechnol. 19 (2001) 365–370.
[10] C.H. Lu, H.H. Yang, C.L. Zhu, A graphene platform for sensing biomolecules, Angew. Chem. Int. Ed. 48 (2009) 4785–4787.
[11] V.V. Didenko, DNA probes using fluorescence resonance energy transfer (FRET): designs and applications, Bio. Tech. 31 (2001) 1106–1121.
[12] J. Brunner, R. Kraemer, Copper (II)-quenched oligonucleotide probes for fluorescent DNA sensing, J. Am. Chem. Soc. 126 (2004) 13626–13627.
[13] H.X. Li, L.J. Rothberg, DNA sequence detection using selective fluorescence quenching of tagged oligonucleotide probes by gold nanoparticles, Anal. Chem. 76 (2004) 5414–5417.
[14] H.L. Li, L. Wang, J.F. Zhai, Coordination polymer nanobelts as an effective sensing platform for fluorescence-enhanced nucleic acid detection, Macromol. Rapid Commun. 32 (2011) 899–904.
[15] L. Yoo, K.-Y. Ahn, J.-Y. Ahn, A simple one-step assay platform based on fluorescence quenching of macroporous silicon, Biosens. Bioelectron. 41 (2013) 477–483.
[16] R.H. Yang, J.Y. Jin, Y. Chen, Carbon nanotube-quenched fluorescent oligonucleotides: probes that fluoresce upon hybridization, J. Am. Chem. Soc. 130 (2008) 8351–8358.
[17] C.H. Lu, H.H. Yang, C.L. Zhu, A graphene platform for sensing biomolecules, Angew. Chem. Int. Ed. 121 (2009) 4879–4881.
[18] H.L. Li, Y.W. Zhang, Y.L. Luo, Nano-C60: a novel, effective, fluorescent sensing platform for biomolecular detection, Small 7 (2011) 1562–1568.
[19] X.F. Wei, L.Y. Zheng, F. Luo, Fluorescence biosensor for the H5N1 antibody based on a metal-organic framework platform, J. Mater. Chem. B 1 (2013) 1812–1817.
[20] L.F. Chen, H.Y. Zheng, X. Zhu, Metal-organic frameworks-based biosensor for sequence-specific recognition of double-stranded DNA, Analyst 138 (2013) 3490–3493.
[21] X. Zhu, H.Y. Zheng, X.F. Wei, Metal-organic framework (MOF): a novel sensing platform for biomolecules, Chem. Commun. 49 (2013) 1276–1278.
[22] M. Eddaoudi, J. Kim, N. Rosi, Systematic design of pore size and functionality in isoreticular metal-organic frameworks and application in methane storage, Science 295 (2002) 469–472.
[23] O.M. Yaghi, M. O'Keeffe, N.W. Ockwig, Reticular synthesis and the design of new materials, Nature 423 (2003) 705–714.
[24] G. Ferey, Hybrid porous solids: past, present, future, Chem. Soc. Rev. 37 (2008) 191–214.
[25] R.E. Morris, P.S. Wheatley, Gas storage in nanoporous materials, Angew. Chem. Int. Ed. 47 (2008) 4966–4981.
[26] K.S. Park, Z. Ni, A.P. Côté, Exceptional chemical and thermal stability of zeolitic imidazolate frameworks, Proc. Natl. Acad. Sci. U.S.A. 103 (2006) 10186–10191.
[27] J.C. Tan, T.D. Bennett, A.K. Cheetham, Chemical structure, network topology, and porosity effects on the mechanical properties of Zeolitic imidazolate frameworks, Proc. Natl. Acad. Sci. U.S.A. 107 (2010) 9938–9943.
[28] N. Chang, Z.-Y. Gu, X.P. Yan, Zeolitic imidazolate framework-8 nanocrystal coated capillary for molecular sieving of branched alkanes from linear alkanes along with high-resolution chromatographic separation of linear alkanes, J. Am. Chem. Soc. 132 (2010) 13645–13647.
[29] A.P. de Silva, H.Q.N. Gunaratne, T. Gunnlaugsson, Signaling recognition events with fluorescent sensors and switches, Chem. Rev. 97 (1997) 1515–1566.
[30] A.F. Gross, E. Sherman, J.J. Vajo, Aqueous room temperature synthesis of cobalt and zinc sodalite zeolitic imidizolate frameworks, Dalton Trans. 41 (2012) 5458–5460.
[31] Y. Pan, H. Li, X.X. Zhang, Large-scale synthesis of ZIF-67 and highly efficient carbon capture using a ZIF-67/glycol-2-methylimidazole slurry, Chem. Eng. Sci. 137 (2015) 504–514.
[32] Y. Cui, Y. Yue, G. Qian, B. Chen, Luminescent functional metal-organic frameworks, Chem. Rev. 112 (2012) 1126–1162.
[33] G.Y. Wang, C. Song, Y. Li, Two luminescent metal-organic frameworks for the sensing of nitroaromatic explosives and DNA strands, J. Mater. Chem. A 2 (2014) 2213–2220.
[34] W. Morris, W.E. Briley, E. Auyeung, M.D. Cabezas, C.A. Mirkin, Nucleic acid-metal organic framework (MOF) nanoparticle conjugates, J. Am. Chem. Soc. 136 (2014) 7261–7264.
[35] Y. Liu, Y.X. Wang, J.Y. Jin, H. Wang, R.H. Yang, W.H. Tan, Fluorescent assay of DNA hybridization with label-free molecular switch: reducing background-signal and improving specificity by using carbon nanotubes, Chem. Commun. 6 (2009) 665–667.
[36] C.K. Wu, Y.M. Zhou, X.M. Miao, L.S. Ling, A novel fluorescent biosensor for sequence-specific recognition of double-stranded DNA with the platform of graphene oxide, Analyst 136 (2011) 2106–2110.
[37] A. Patterson, F. Caprio, A. Vallée-Bélisle, D. Moscone, K.W. Plaxco, G. Palleschi, F. Ricci, Using triplex-forming oligonucleotide probes for the reagentless, electrochemical detection of double-stranded DNA, Anal. Chem. 82 (2010) 9109–9115.
[38] L.f. Chen, H. Zheng, X. Zhu, Z. Lin, L. Guo, B. Qiu, G. Chen, Z. Chen, Metal-organic frameworks-based biosensor for sequence-specific recognition of double-stranded DNA, Analyst 138 (2013) 3490–3493.